Supporting Information

Agglomeration of *Escherichia coli* with positively charged nanoparticles can lead to artifacts in a standard *Caenorhabditis elegans* toxicity assay

Shannon K. Hanna [#*], Antonio Montoro Bustos, Alexander W. Peterson, Vytas Reipa, Leona D. Scanlan†, Sanem Hosbas Coskun, Tae Joon Cho, Monique E. Johnson, Vincent A. Hackley, Bryant C. Nelson, Michael R. Winchester, John T. Elliott, Elijah J. Petersen

Materials Measurement Laboratory, National Institute of Standards and Technology, 100 Bureau Drive, Gaithersburg, MD 20899-8313

[#] Current address: Center for Tobacco Products, Food and Drug Administration, 10903 New Hampshire Avenue, Silver Spring, MD 20993

† Current address: Department of Pesticide Regulation, California Environmental Protection Agency, 1001 I Street, Sacramento, CA 95814

* Corresponding author: hanna.shannonk@gmail.com

8 pages total, 2 figures and 2 tables

Supplemental methods

Zeta Potential and Dynamic Light Scattering Measurements

Zeta potential (Z-P) measurements were operated in 173° backscatter mode with a laser wavelength of 633 nm using a palladium dip cell with disposable cuvettes (Brandtech, Inc., Essex, CT) and applying the Smoluchowski equation for thin double layers. Measurements were taken in DI water or half-strength M9, the medium used in ISO 10872 and described in the main text. Most samples were diluted 10:1 (v/v) so that the final concentration was ≈ 5 mg/L. The medium was filtered first using a 0.8/0.2 µm polyethersulfone syringe filter (Acrodisc^{R} PF, PALL Cooperation, Ann Abor, MI) to remove particles that could interfere with the zeta potential measurements. Triplicate samples were analyzed for each particle tested, and each sample was measured three times (each measurement was conducted with up to 100 sub-runs). Agglomeration was observed for some samples after the Z-P measurements as indicated by a change in color of the suspension in the cuvette. For these samples, the number of sub-runs was decreased to a maximum of 30. Outlier results (less than 2 % of total ZP measurements) were removed using the Grubb's test (GraphPad Prism). Batch mode DLS procedures followed NIST-NCL Protocol[1] to measure the z-average diameter. Samples for DLS measurements were prepared similarly except the size was only measured in DI water. Five measurements were made of a single sample (each measurement was conducted with 11 up to 100 sub-runs). Z-P and z-average size were reported as a mean of no less than three (for Z-P) and five measurements (for DLS) plus or minus one standard deviation for each replicate; triplicate replicates were tested for each Z-P measurement while a single replicate was measured for the DLS measurements. All Z-P and DLS measurements were conducted at (20 ± 0.1) °C unless noted otherwise.

Axenic Medium

Axenic medium was prepared in a sterile hood as described by Samuel et al.[2] and frozen for later use. Components are listed in Table S1. Double concentrated axenic medium (2X) was prepared by eliminating half of the sterile, deionized water from the ingredients.

ISO assay (modified and reprinted with permission from Hanna et al.[3])

The test wells were prepared by adding 500 µL of the test material and 500 µL of the *E. coli* suspension to each well. J1 nematodes for the toxicity tests were obtained using a standard bleaching protocol in which a mixed culture of nematodes was exposed to a sodium hypochlorite and sodium hydroxide mixture for 10 min, washed with sterile water three times and the eggs were allowed to hatch in sterile water overnight. Bleached nematodes were only J1 stage, as development is arrested when a food source is absent. Ten J1 nematodes were added to each well of a 12-well plate and the test was initiated by placing the plates into a 20 °C incubator, in the dark, and leaving them undisturbed for 96 h. All J1 nematodes not used in the test were stained with Rose Bengal (500 µL of a 300 mg L^{-1} stock was added to 5 mL), heated at 80 °C for 10 min to kill and straighten them, 30 individuals were measured, as described in the following section, to determine the initial nematode length. At the end of the assay, 200 μL of a 300 mg L^{-1} stock of Rose Bengal was added to each well and the plate was heated at 80 °C for 10 min to kill and straighten all of the nematodes. Plates were allowed to cool for at least 1 h prior to imaging. All plates were stored at 4 °C and imaged within one week after the experiment concluded. Details for imaging of the wells after the ISO and axenic assays, and calculation of the percentage inhibition for growth and reproduction and provided in the following sections.

Imaging optimization and processing, nematode length measurements, and reproductive counts *(modified and reprinted with permission from Hanna et al.[3])*

Whole-well imaging improved the reliability of nematode measurements by providing a system by which a line can be placed on each nematode and their length determined through software instead of manually estimating length based on a scale bar under a microscope. However, whole-well imaging also introduced additional sources of variability and required optimization of various parameters. We optimized the amount of Rose Bengal to add to the wells by adding increasing concentrations to wells and measuring the difference in intensity between a nematode and the background. We achieved the greatest contrast at 60 mg L^{-1} of Rose Bengal. We imaged each well of the 12-well plates using a CoolSNAPHQ2 CCD camera (Photometrics, Tucson, AZ) coupled to an automated Zeiss microscope (Axio Vert.A1, Carl Zeiss Microscopy, Oberkochen, Germany) with Zen software (Carl Zeiss Microscopy, 2012 Blue Edition). The microscope was calibrated using a stage micrometer (Electron Microscopy Services) at 5 x prior to the study. Transmitted light intensity was set to 3.7 V and exposure time was 2 ms. Whole-well imaging was improved by addition of 1 mL of light paraffin oil (Taylor Scientific, St. Louis, MO, USA) to the top of the well, which reduced darkening generated by the water meniscus. The plate was calibrated by finding and focusing on the edges of the wells. A focus surface was defined by fixing five points in each well. While adding additional points would improve focus, we found that five points provided sufficient focus to allow identification and measurement of worms. Using the calibration and focal points, entire wells were imaged (see Fig. 2). Images were exported as .tiff files and adult hermaphrodites were measured (males, if present, were excluded) and young were counted using ImageJ (1.47v, Wayne Rasband, NIH, USA) with the scale based on the stage micrometer calibration. Total nematode length was measured using a segmented line tracing the center of the nematode from the tip of the head to the end of the tail. Young were counted in one quarter of each well to estimate total well reproduction. While issues such as stitching, poor focus, and interferences may impact image quality, the automated imaging system helped to overcome many of those problems and increased the quality of our data as discussed in depth in Hanna et al. 2016.[3]

Calculation of growth and reproduction inhibition (modified and reprinted with permission from Hanna et al.[3])

Mean growth of nematodes in each well was calculated by subtracting the mean length of adult hermaphrodites by the mean length of J1 nematodes measured at the start of the assay. Inhibition of growth (G_I) was calculated for each nematode as follows:

$$G_I = 100 - \frac{L_F - L_I}{G} * 100$$

where L_F is final length of the individual nematode at the end of the assay, L_I is the mean initial J_1 length at the start of the assay, and G is the mean growth of the control nematodes during the assay. Inhibition of reproduction (R_I) was calculated for each well as follows:

$$R_I = \frac{R_C - R_W}{R_C} * 100$$

where R_C is the mean reproduction per adult hermaphrodite found for the control wells and R_W is the reproduction per adult hermaphrodite found in the test well. EC50 for growth and reproduction was determined using a four-parameter logistic function in GraphPad Prism (V 6.04, GraphPad Software, Inc.).

Reference

1. V. A. Hackley and J. D. Clogston, Measuring the size of nanoparticles in aqueous media using batch-mode dynamic light scattering. NIST-NCL Joint Assay Protocol, PCC-1. Version 1.2. http://dx.doi.org/10.6028/NIST.SP.1200-6, 2015.

2. T. K. Samuel, J. W. Sinclair, K. L. Pinter and I. Hamza, Culturing Caenorhabditis elegans in axenic liquid media and creation of transgenic worms by microparticle bombardment. *J. Vis. Exp.* **2014,** *(90)*, e51796.

3. Hanna, S. K.; Cooksey, G. A.; Dong, S.; Nelson, B. C.; Mao, L.; Elliott, J. T.; Petersen, E. J., Feasibility of using a standardized Caenorhabditis elegans toxicity test to assess nanomaterial toxicity. *Environmental Science: Nano* **2016,** *3*, 1080-1089.

PS ENPs

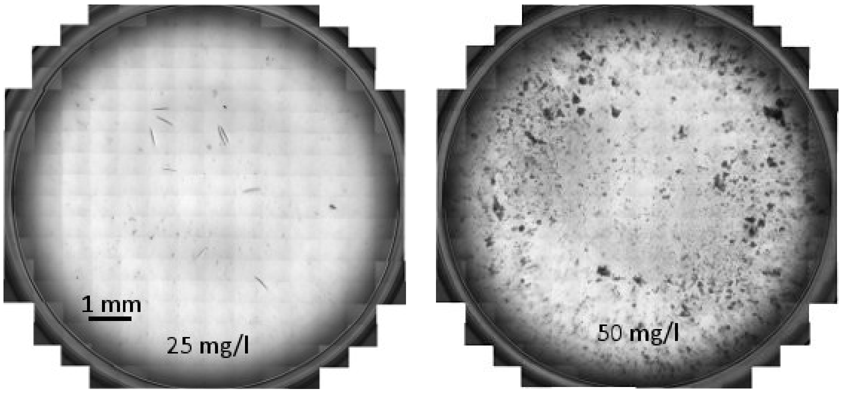

30 nm bPEI Au ENPs

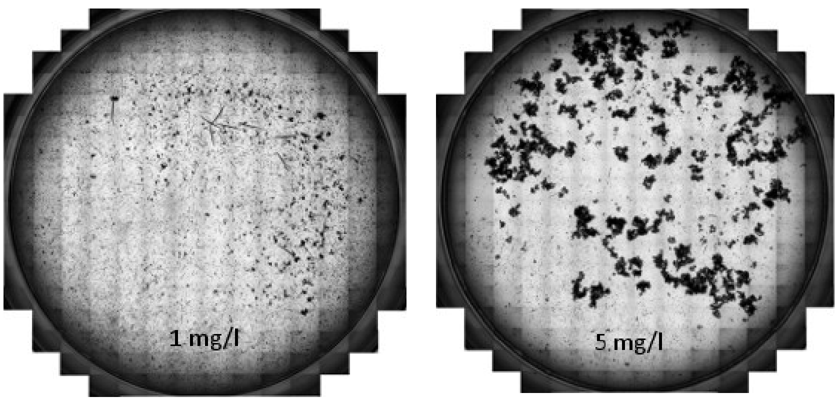

Figure S1. Positively charged ENPs such as 30 nm bPEI Au ENPs and PS ENPs produced large agglomerates, which appeared to increase with increasing concentration of ENPs. These images were taken of wells from the 12-well plates after conducting the ISO assay.

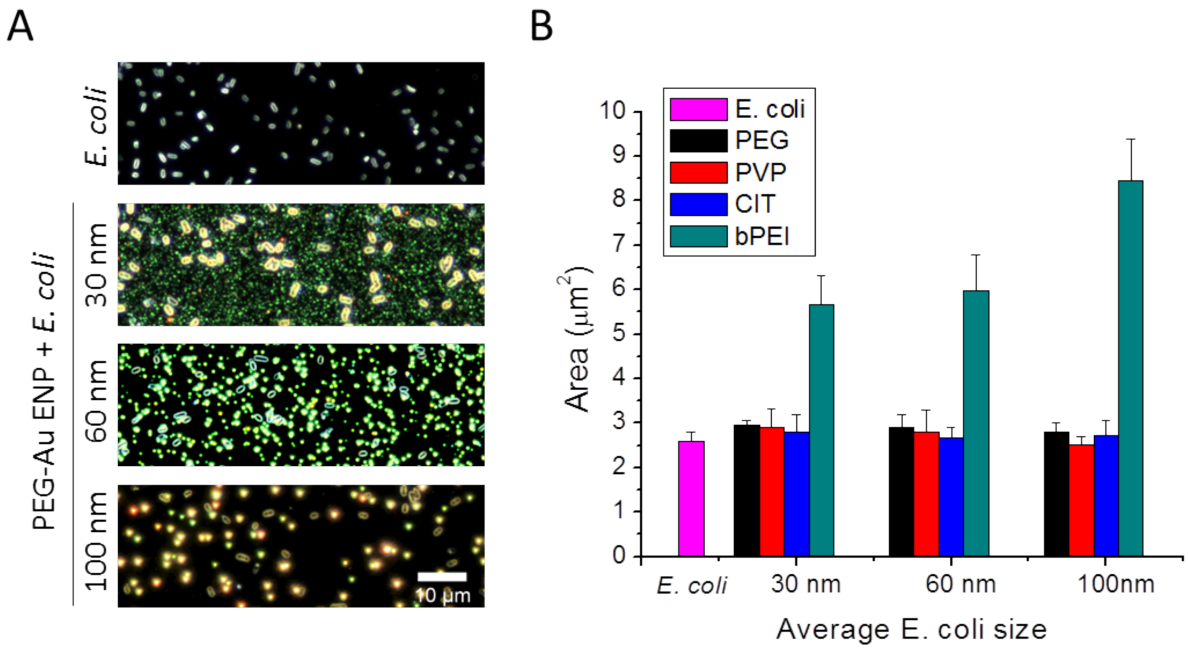

Figure S2. Enhanced darkfield imaging of neutral or negatively charged coated Au ENPs incubated with *E. coli* reveals no observable interaction or aggregation. A) Representative images of *E. coli* alone and exposed to PEG coated Au ENPs of size 30, 60, and 100 nm diameter. Visual inspection reveals both *E. coli* and Au ENPs remain as single dispersed particles with no noticeable interactions. A scale bar of 10 µm is provided in the lower right corner. B) Image analysis of bacteria size results in average area of *E. coli* reported for each Au ENP size (30 nm, 60 nm, 100 nm) and coating (PEG, PVP, CIT, bPEI). No observable change in *E. coli* size/aggregation is observed, within the error of measurement, for the neutral/negatively charged gold particle coatings: PEG, PVP, or CIT. In contrast, the positively charged bPEI coated Au ENPs show an immediate change in average bacteria particle (agglomerate) size at the 0 min time point after mixing shown here. Error bars represent 1 standard deviation.

Table S1. Composition of Axenic Medium (as described by Samuel et al.[2])

Component	**Volume**
Choline diacid citrate (2 mM)	10 mL
Vitamin and growth factor mix	10 mL
Solution 1	
Sterile, deionized water	60 mL
N-acetyl-α-D-glucosamine	0.15 g
DL-alanine	0.15 g
Nicotinamide	0.075 g
D-pantethine	0.0375 g
DL-pantothenic acid, hemi calcium salt	0.075 g
Folic acid	0.075 g
Pyridoxamine 2HCl	0.0375 g
Pyridoxine HCl	0.075 g
Flavin mononucleotide, sodium salt	0.075 g
Thiamine hydrochloride	0.075 g
Solution 2	
1 N KOH	5 mL
p-aminobenzoic acid	0.075 g
D-biotin	0.0375 g
Cyanocobalamin (B12)	0.0375 g
Folinic acid, calcium salt	0.0375 g
Nicotinic acid	0.075 g
Pyridoxal 5-phosphate	0.0375 g
Solution 3	
Ethanol	1 mL
(±) α-L-lipoic acid, oxidized form	0.0375 g
Combine solutions 1, 2, and 3 and bring the final volume to 100 mL with sterile, deionized water	
myo-Inositol (2.4 mM)	10 mL
Hemin chloride (2 mM in 0.1 N NaOH pH 8.0)	10 mL
Sterile deionized water	250 mL
Nucleic acid mix:	20 mL
Sterile, deionized water	60 mL
Adenosine 5' -monophosphate, sodium salt	1.74 g
Cytidine 5' -phosphate	1.84 g
Guanosine 2' - and 3' -monophosphate	1.82 g
Bring solution to 100 mL	
Mineral Mix:	100 mL
$MgCl_2 \cdot 6H_2O$	4.1 g
Sodium citrate	2.9 g
Potassium citrate monohydrate	4.9 g
$CuCl_2 \cdot 2H_2O$	0.07 g
$MnCl_2 \cdot 4H_2O$	0.2 g

$ZnCl_2$	0.1 g
$Fe(NH_4)_2(SO_4)_2{\bullet}6H_2O$	0.6 g
$CaCl_2{\bullet}2H_2O$ (add last)	0.2 g
Lactalbumin enzymatic hydrolysate (170 mg/mL)	20 mL
Essential Amino Acid Mix	20 mL
Non-essential Amino Acid Mix	10 mL
KH_2PO_4 (450 mM)	20 mL
D-Glucose (1.5 M)	50 mL
HEPES, sodium salt (1 M)	10 mL
Sterile deionized water	250 mL
Cholesterol (5 mg mL in ethanol)	1 mL
Ultra-pasteurized skim milk (add immediately before use)	200 mL

Table S2. Properties of ENPs tested

Product Name	Surface coating	Size (nm)	Mass concentration of stock (mg L^{-1})[g]	Zeta potential in DI Water[h]	Zeta potential in 50% M9[h]
30 nm bPEI Au ENPs	bPEI	30.9 ± 2.9 (TEM),[a] 45.0 ± 0.8 (DLS)[b]	52	43.3 ± 4.4	12.2 ± 2.0
60 nm bPEI Au ENPs	bPEI	63.7 ± 7.3 (TEM),[a] 91.1 ± 2.1 (DLS)	52	51.7 ± 1.5	10.3 ± 1.4[i]
100 nm bPEI Au ENPs	bPEI	98.1 ± 10.1 (TEM),[a] 101 ± 2 (DLS)	52	57.4 ± 1.2	12.2 ± 2.6
30 nm Citrate Au ENPs (NIST 8012)	Sodium Citrate	28.6 ± 0.9 (DLS),[b] 26.9 ± 0.1 (SEM)[b]	48.17 ± 0.33	-40.4 ± 1.4	-43.6 ± 3.1
60 nm Citrate Au ENPs (NIST 8013)	Sodium Citrate	56.6 ± 1.4 (DLS),[b, c] 54.9 ± 0.4 (SEM)[b]	51.86 ± 0.64	-42.5 ± 3.2	-30.3 ± 1.1
100 nm Citrate Au ENPs	Sodium Citrate	104 ± 13 (TEM),[a] 101 ± 2 (DLS)	52	-51.3 ± 0.9	-33.8 ± 4.7
30 nm PEG Au ENPs	mPEG 5 kDa	32.7 ± 11.0 (TEM),[a] 51.7 ± 1.1 (DLS)	51	-16.8 ± 3.3	-8.51 ± 5.57
60 nm PEG Au ENPs	mPEG 5 kDa	65.3 ± 12.3 (TEM),[a] 69.6 ± 1.3 (DLS)	53	-31.3 ± 3.1	-7.05 ± 2.45
100 nm PEG Au ENPs	mPEG 5 kDa	105 ± 14 (TEM),[a] 108 ± 2 (DLS)	54	-36.1 ± 4.7	-13.1 ± 1.2
30 nm PVP Au ENPs	PVP	29.7 ± 2.6 (TEM),[a] 46.5 ± 1.0 (DLS)	50	-29.0 ± 2.2	-11.2 ± 1.6
60 nm PVP Au ENPs	PVP	55.9 ± 7.9 (TEM),[a] 85.6 ± 1.0 (DLS)	54	-33.3 ± 2.5	-8.07 ± 1.93
100 nm PVP Au ENPs	PVP	100.0 ± 7.4 (TEM),[a] 124 ± 2 (DLS)	52	-28.0 ± 3.5	-5.58 ± 1.85
10 nm PCD Au ENPs	Dendrons	16.3 ± 0.5 (DLS), 7.2 ± 2.1 (TEM)[d]	330 ± 1	-2.93 ± 1.71	-10.1 ± 1.5
2 nm Si ENPs	Amine	1.9 ± 0.3 (DLS), 1.9 ± 0.2 (TEM)[e]	90 ± 1[e]	13.8 ± 1.0	1.1 ± 0.6
55 nm PS ENPs	Amine	56.6 ± 0.9 (DLS), 51 ± 9 (SEM)[f]	100 000[f]	32.9 ± 2.2	32.3 ± 3.3

[a] Values are the mean ± 1 standard deviation of at least five measurements of a single sample for DLS measurements or 100 particles for TEM measurements. Transmission electron microscopy (TEM) sizes were provided by the manufacturer.

[b] Values are those provided in the Report of Investigation for reference material 8012 and 8013 and indicate the mean ± expanded uncertainty. The number of replicates tested for these analyses are in the Reports of Investigation.

[c] In addition to the data provided in the Report of Investigation, this sample was also analyzed on the same day as the other DLS measurements. This analysis yielded a result of 60.8 ± 0.9 (mean ± 1 standard deviation of at least three replicates).

[d] Data is from Cho, T. J.; MacCuspie, R. I.; Gigault, J.; Gorham, J. M.; Elliott, J. T.; Hackley, V. A., Highly Stable Positively Charged Dendron-Encapsulated Gold Nanoparticles. *Langmuir* **2014,** *30* (13), 3883-3893.

[e] The TEM value is from the NIST Report of Investigation for RM 8027. The TEM data is the mean ± 1 standard deviation of 560 particles. The DLS data is from NIST special publication 1200-12. The DLS and Si concentration data are the mean ± 1 standard deviation of three measurements.

[f] Data is from Elliott, J. T.; Rösslein, M.; Song, N. W.; Blaza, T.; Kinsner-Ovaskainen, A.; Maniratanachote, R.; Salit, M. L.; Petersen, E. J.; Sequeira, F.; Lee, J.; Rossi, F.; Hirsch, C.; Krug, H. F.; Suchaoin, W.; Wick, P., Toward achieving harmonization in a nano-cytotoxicity assay measurement through an interlaboratory comparison study. *Altex* **2017,** *34* (2), 389-398.

[g] Au mass fraction provided by the manufacturer for the commercial materials and in the Report of Investigation for reference material 8012 and 8013, respectively. For RM 8012 and RM 8013, the expanded uncertainty (95 % confidence interval) is calculated according to the ISO/JCGM Guide. For the PCD AuENPs, the values are mean ± 1 standard deviation (n=3) measured using inductively coupled plasma-mass spectrometry.

[h] Values are the mean ± 1 standard deviation of at least three replicates. Standard deviation values represent the propagated error for the measurements of the replicates and the standard deviation of the runs in each replicate measurement.

[i] For some samples analyzed on one day for this sample, agglomeration was observed followed by a rapid change in the zeta potential value. This result was observed using two different Malvern zetasizer instruments. These results were excluded from calculating the average values. The result from the second zetasizer instrument was 10.5 ± 1.1 indicating the reproducibility of this result; this value is the mean ± 1 standard deviation of three replicates. Standard deviation values represent the propagated error for the measurements of the replicates and the standard deviation of the runs in each replicate measurement.